Short communication

Effects of ball-milling conditions on dehydrogenation of Mg(NH$_2$)$_2$–MgH$_2$

Jianjiang Hu [a], Zhitao Xiong [a], Guotao Wu [a], Ping Chen [a,*],
Kenji Murata [b], Ko Sakata [b]

[a] *Department of Physics, National University of Singapore, Singapore 117542, Singapore*
[b] *The Institute of Applied Energy, Tokyo, Japan*

Available online 19 May 2006

Abstract

The dependence of chemical reaction between Mg(NH$_2$)$_2$ and MgH$_2$ on the ball-milling conditions has been investigated. While the decomposition of the component Mg(NH$_2$)$_2$ resulted in gaseous products consisting mainly of ammonia, the mixtures of Mg(NH$_2$)$_2$–MgH$_2$ prepared by ball-milling released H$_2$ at temperatures as low as 65 °C. In addition, the increase in ball-milling time can effectively suppress the ammonia evolution during the thermal treatment. The conversion of the amide and hydride to imide-like structure was demonstrated by FTIR and XRD characterization. A total amount of 4.8 wt.% of H$_2$ could be released from the investigated system.
© 2006 Elsevier B.V. All rights reserved.

Keywords: Magnesium amide; Magnesium hydride; Ball-milling time; Imide formation; Hydrogen desorption

1. Introduction

The establishment of metal nitrides and imides as potential hydrogen storage materials has considerably widened the material scope for hydrogen storage media [1–4]. Interesting systems have been designed and developed, using the concept of affinitive combination of proton cation H$^{\delta+}$ in amide and H$^{\delta-}$ in hydride. Successful examples are LiNH$_2$–LiH [2], Mg(NH$_2$)$_2$–LiH [5] and Mg(NH$_2$)$_2$–NaH systems [6]. Studies using similar concept have also been reported by other groups as well [7,8].

Among the amide–hydride systems, Mg(NH$_2$)$_2$–MgH$_2$ appears attractive to us because it possesses high hydrogen content (six hydrogen atoms or 7.3 wt.% at 1:1 molar ratio). It is well-known that MgH$_2$ is an ionic type hydride. Therefore, the chemical reaction between Mg(NH$_2$)$_2$ and MgH$_2$ is expectable. Our previous results did reveal the hydrogen desorption from the aforementioned mixture [9,10]. More recently, Nakamori et al. [11] also investigated Mg(NH$_2$)$_2$ and MgH$_2$ with molar ratios of 1:1 and 1:2. However, only ammonia rather than H$_2$ was detected, which resembles the thermal decomposition of magnesium amide alone. The authors concluded that the slow

kinetics of the reaction between MgH$_2$ and ammonia hindered the H$_2$ generation. Based on the different experimental observations and the high potential for Mg–N–H system as hydrogen storage material, detailed investigations are necessary.

Ball-milling is a widespread method in the preparation of alloys and solid phase mixtures [12–16]. It is also a very convenient way for conducting solid state reactions [14]. We have detected chemical reactions among the solid powders inside the milling jar, particularly the interactions between metal amides and hydrides or hydride complexes. In the present work, we prepared the Mg(NH$_2$)$_2$–MgH$_2$ mixtures using a planetary ball-mill. The effects of milling time on the samples were studied. Fourier transform infrared (FTIR) and X-ray diffractometry (XRD) were used for the characterization of structural changes. GC–MS was used for ammonia detection during the temperature-programmed-desorption (TPD) treatments.

2. Experimental

2.1. Materials

MgH$_2$ was a product of Alfa Aesar with 98% purity. Mg(NH$_2$)$_2$ was synthesized in house by reacting Mg powder (97%, Riedel-De Haen) with 120 psi ammonia at about 300 °C. The structure of Mg(NH$_2$)$_2$ was confirmed by X-ray diffraction.

Table 1
Dependence of pressure increase in milling jar on milling time

Ball-milling time (h)	Pressure increase (psi)	Calculated number of H atoms released per $Mg(NH_2)_2$–MgH_2	wt.%[a]
5	0	0	0
11	2	0.04	0.06
17	10	0.22	0.25
24	23	0.51	0.69
72	71	1.58	2.14

[a] After correction with purity of starting materials.

2.2. Ball-milling treatment

The ball-milling of $Mg(NH_2)_2$ with MgH_2 at 1:1 molar ratio was conducted on a Fritsch planetary ball-mill at 200 rpm. The milling jars were equipped with gas valves for the measurement of pressure increase caused by gas release during ball-milling. The gas generated during ball-milling was analyzed by a mass spectrometer (Hiden Analytical) and an ammonia sensitive reagent (aqueous $Co(NO_3)_2$ solution).

2.3. Methods

A home-made apparatus was used for temperature-programmed-desorption (TPD) experiments. Detailed procedure can be found elsewhere [17]. About 100 mg sample was used for each experiment. Tail gas was introduced to an MS–GC combined system for ammonia detection.

A gas reaction controller provided by Advanced Materials Co. was applied to measure the amount of hydrogen released. About 500 mg sample was used for each measurement. The system was evacuated at room temperature and the sample holder was heated from 20 °C at 2 °C min^{-1} to the desired temperature.

FTIR measurements were conducted on a Perkin-Elemer FTIR-3000 unit in DRIFT mode.

X-ray diffraction profiles were obtained on a Bruker D8-advance X-ray diffractometer with Cu Kα radiation.

3. Results and discussion

3.1. Results of TPD and ammonia monitoring

Gases were found to be generated during the ball-milling process. Analysis of the gaseous products by MS and cobalt nitrate solution revealed that hydrogen was the only product. Table 1 lists the pressure increase measured after certain period of ball-milling. Below 5 h there was no pressure increase detected in the milling jar which could be related to the particle size of the two reactants. As the ball-milling proceeds, the particle size of the two reacting species decreases. When the particle size or specific surface area reaches a certain value, the reaction in the solid state takes place.

Fig. 1 is the plot of H_2 pressure increase in milling jar against milling time. The H_2 generation or reaction rate accelerated after about 15 h and declined after 40–50 h. This may be explained by the changes in the particle size and concentration of amide
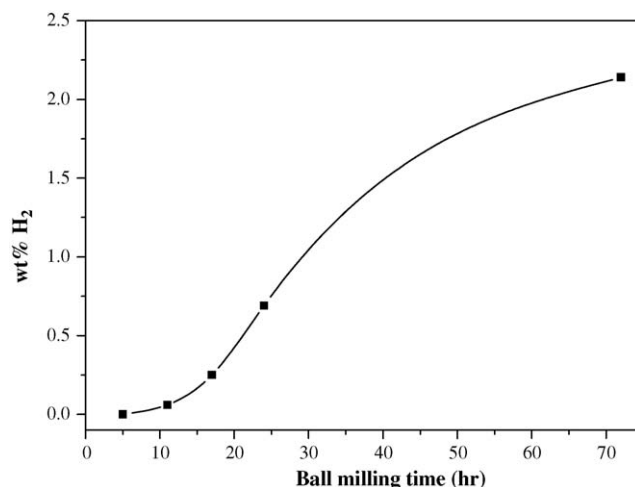

Fig. 1. Hydrogen release dependence on ball-milling time.

and hydride during ball-milling. According to the rate law of chemical reaction, the reaction rate is proportional to the concentration of reactant. When the threshold specific surface area is reached, the reaction rate is determined by the reactant concentration. The H_2 generation during the ball-milling process clearly evidences the readiness of the reaction between amide and hydride.

Magnesium amide $Mg(NH_2)_2$, one of the components in the mixture, decomposes to magnesium imide (MgNH) and ammonia upon heating to 360 °C. The generation of NH_3 began at about 200 °C [7]. The TPD curve of $Mg(NH_2)_2$ exhibits a peak at 384 °C in our experiment (not shown) which can be attributed to the NH_3 generation. The TPD curve of the MgH_2 alone shows the beginning of the hydrogen generation at 390 °C and a peak at 426 °C at a heating rate of 2 °C min^{-1} (not shown).

Shown in Fig. 2 are the TPD curves of the samples ball-milled for different times. It can be seen that H_2 was released at temperature below 100 °C. For the sample of 5 h milling time (not shown), no H_2 was desorbed until 200 °C. In contrast, H_2 signal was emerging from samples milled for 11 h or longer, which started at about 65 °C. The sample milled for 11 h gives a complicated desorption process, while the rest three samples show a major peak at around 300 °C followed by a sharp peak at 400 °C. It was reported that powdery MgH_2 alone could be activated for H_2 desorption at relatively low temperature after ball-milling to nanometer scale. The peak temperature of H_2 desorption was lowered by 64 °C from 430 to 366 °C after 20 h ball-milling [18]. The H_2 signal at low temperature observed in our work did not likely originate from the H_2 desorption of milled MgH_2, but rather due to the chemical reaction between corresponding amide and hydride, which takes place only after certain threshold value of ball-milling.

NH_3 release is a serious issue in using N-containing compounds as H_2 storage materials. It would on the one hand lower the H_2 storage efficiency and at the same time impair the system reversibility due to the possible changes in stoichiometry. Shown in Fig. 3 are curves obtained from GC–MS for the NH_3 detection of the ball-milled samples. Two steps of NH_3 release can be identified. The first step before 350 °C starts from about 200 °C
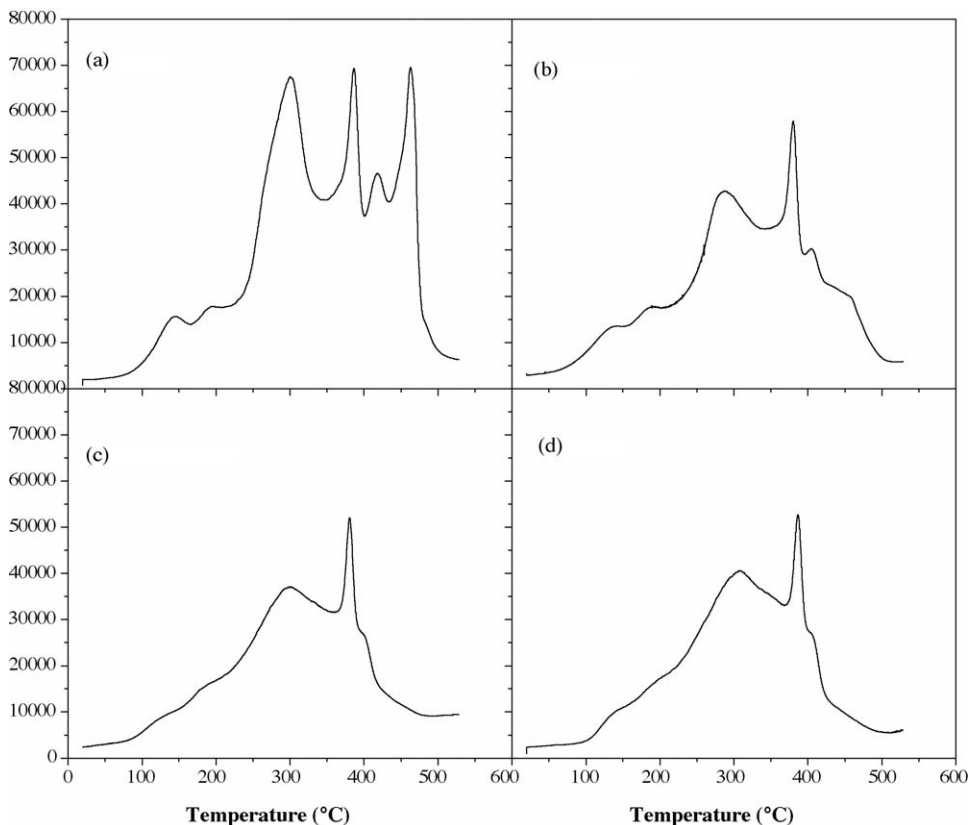
Fig. 2. TPD curves of samples milled for (a) 11 h, (b) 17 h, (c) 24 h and (d) 72 h.

followed by a sharp NH_3 release peak at around 400 °C. However, the signal intensity of NH_3 release at the first step decreased with the milling time. For the sample with the longest milling time (72 h), the NH_3 release in the first step was effectively suppressed. The majority of NH_3 release was detected only at temperature above 350 °C, which is obviously different from the observation made by Nakamori et al. [11]. We attribute the alternation in the thermal decomposition behavior, compared to the individual component, to the chemical reaction of the amide and hydride during ball-milling process. From Figs. 2 and 3
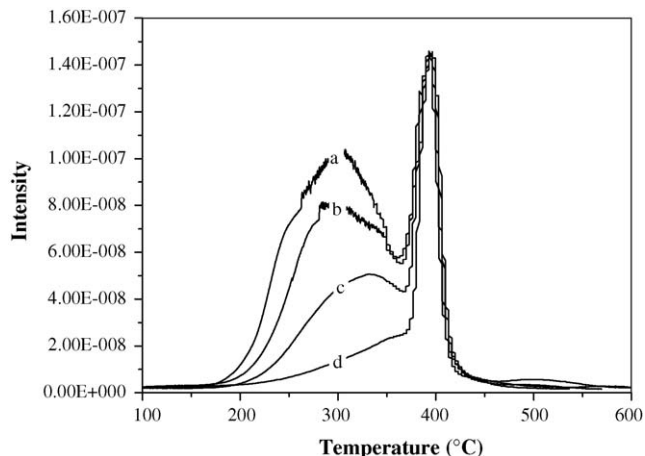

Fig. 3. NH_3 monitoring by GC–MS of samples milled for (a) 11 h, (b) 17 h, (c) 24 h and (d) 72 h.

we can see that hydrogen desorption should be performed before 200 °C for the 11 h milled sample and before 310 °C for the 72 h billed sample, respectively, in order to prevent NH_3 generation.

From the behaviors of H_2 and NH_3 release, it can be seen that the ball-milling is not simply a mechanical mixing process, but rather a way of promoting in situ chemical synthesis. The properties of the ball-milled samples are more likely determined by the chemical reactions or the products of the chemical reactions which concurrently take place among the milling components during the ball-milling. The ball-milling seems to have increased the probabilities of the encounter of the proton cation $H^{\delta+}$ in amide and $H^{\delta-}$ in hydride, leading to the combination reaction.

3.2. FTIR spectra

FTIR spectra of samples milled for different periods of time are shown in Fig. 4. The typical absorbances at 3271/3326 cm^{-1} of the amide ions in $Mg(NH_2)_2$ [19] can still be seen even in the sample with the longest milling time (72 h), indicating the presence of $Mg(NH_2)_2$. However, the intensity decreased with the milling time implies its progressive conversion. A new broad absorbance appeared at a lower wavenumber (3196 cm^{-1}) with extended milling and its intensity increased with the milling time.

A series of TPD experiments were carried out on the sample milled for 11 h and the FTIR spectra thereof are shown in Fig. 5.
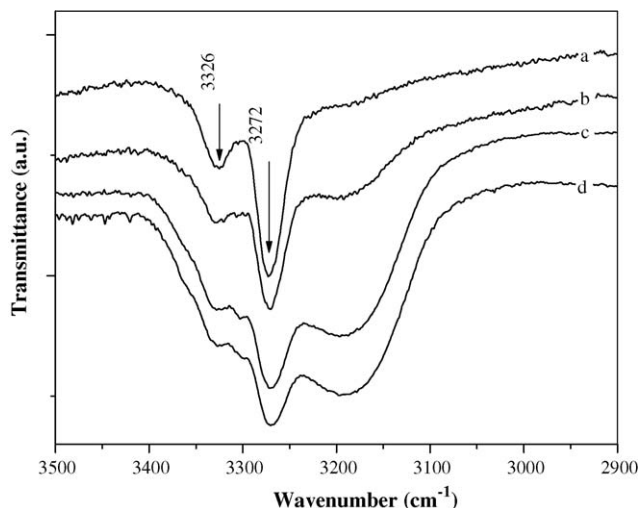
Fig. 4. FTIR spectra of as-milled samples (a) 11 h, (b) 17 h, (c) 24 h and (d) 72 h.

Fig. 6. FTIR spectra of 72 h milled sample after TPD treatments.

Similarly to the milling effect, the absorbance at $3196\,\text{cm}^{-1}$ became stronger with the increase in TPD temperature. But it was eliminated by further heating to $500\,^{\circ}\text{C}$ (not shown). Spectra of sample milled for 72 h and subsequently treated at different temperatures in TPD experiments are shown in Fig. 6. After holding the temperature at $314\,^{\circ}\text{C}$ for 420 min, the residual amide was hardly to be recognized in the FTIR spectrum, and there was only the new broad absorbance in this range. In the Ref. [19], the IR of magnesium imide MgNH showed vibration absorbances at 3251 and $3199\,\text{cm}^{-1}$. The absorbance at $3251\,\text{cm}^{-1}$ was difficult to distinguish in our work due to the strong broad absorbance. We assume that the broad absorbance at $3196\,\text{cm}^{-1}$ was attributed to MgNH or a MgNH-like structure. Therefore, we believe that H_2 was released from the reaction between $Mg(NH_2)_2$ and MgH_2 with an imide-like structure being formed.
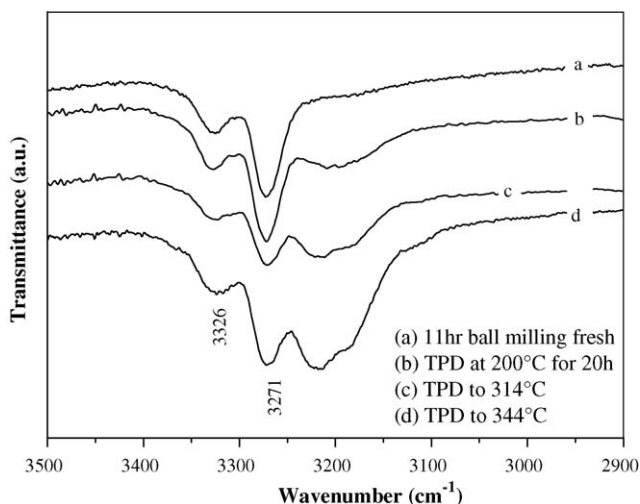
3.3. XRD results

XRD measurements (Figs. 7–9) were performed for the three sets of samples subjected to FTIR measurements. Although the MgH_2 phase can be seen for all the four samples with different milling time, two broad peaks centered at around 41° and 61°, respectively, increased gradually with the milling time (Fig. 7) in the same order as the imide-like broad absorbance in FTIR spectra (Figs. 4–6). MgH_2 phase was predominant in the as-prepared 11 h milling sample (Fig. 8(a)). However, the diffractions at 41° and 61° emerged after TPD treatment at $314\,^{\circ}\text{C}$ and was enhanced at TPD $344\,^{\circ}\text{C}$ (Fig. 8(b) and (c)). After TPD treatment at $600\,^{\circ}\text{C}$, only Mg_3N_2 phase can be identified (Fig. 8(d)). For the 72 h milled sample the diffractions at 41° and 61° were already strong in the as-prepared sample (Fig. 9(a)). After TPD at $314\,^{\circ}\text{C}$, the MgH_2 phase was substantially reduced (Fig. 9(b)).
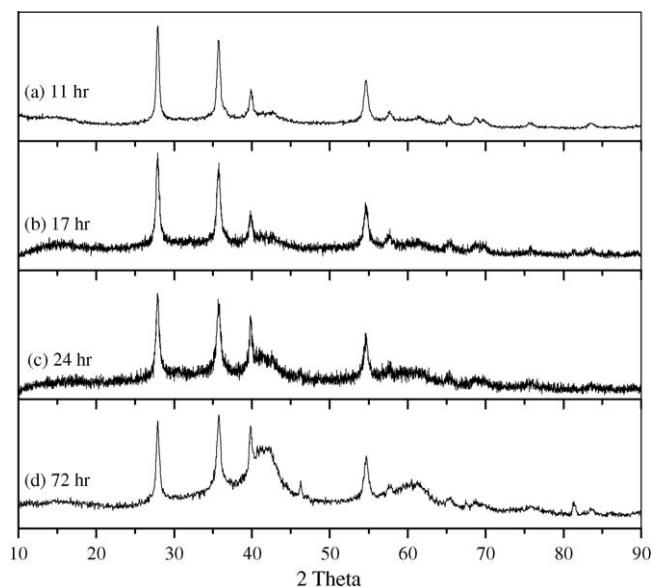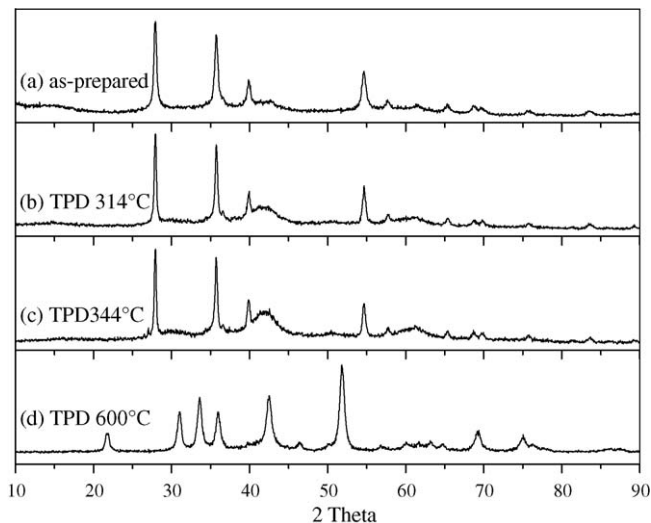

Fig. 5. FTIR spectra of 11 h milled sample after TPD treatments.

Fig. 7. XRD patterns of as-milled samples.

Fig. 8. XRD patterns of 11 h milled sample after TPD treatments.

Fig. 10. Volumetric release measurements for 11 and 72 h milled samples.

3.4. Volumetric release measurements

The volumetric release was carried out for samples of 11 and 72 h milling, with the sample holder being heated from 20 °C at 2 °C min^{-1}. The utmost temperature for H_2 release was determined by the temperature at which ammonia was generated. Since ammonia was released early at 200 °C for the 11 h milling sample, the release was stopped at 200 °C. A sparse amount of 0.7 wt.% H_2 was measured (Fig. 10).

For the 72 h milling sample, H_2 desorption consists of three parts. The first part was 2.1 wt.% released during ball-milling. During the volumetric release, about 2.2 wt.% was released from 20 to 310 °C. Additional 0.6 wt.% H_2 was released after keeping the temperature at 310 °C. This means that more than three H atoms were released before the second step of TPD experiment (see Figs. 2 and 3). Together with the TPD, MS and XRD results, the ammonia release in the higher temperature range is described as follows:

$$Mg(NH)_x \rightarrow \ Mg_3N_2 + NH_3$$

Summarizing the above results, the total amount of H_2 release for the system was 4.8 wt.%, which is equivalent to four H atoms desorbed per one $Mg(NH_2)_2$–MgH_2. As such, we would describe the H_2 desorption with the following reaction equation:

$$Mg(NH_2)_2 + MgH_2 = 2MgNH \ + \ 2H_2$$

$$H \, content \ = \ 4.88 \, wt.\%$$

Holding the temperature at 314 °C further lowered the content of MgH_2 phase. At the same time, the Mg_3N_2 phase became discernable (Fig. 9(c)), and finally affirmed at 600 °C (Fig. 9(d)).

The broad diffraction peaks at 41° and 61° are difficult to assign to a known structure using the database of the XRD instrument. However, taking into account of the FTIR results, we would connect the diffraction patterns to MgNH or MgNH-like structure.

It can be seen from the above results that both components of the mixture still exist after ball-milling. We have observed that the crystalline $Mg(NH_2)_2$ itself becomes amorphous readily after ball-milling, which can hardly be identified by XRD. The gradual consumption of $Mg(NH_2)_2$ and MgH_2 with H_2 release, as evidenced by FTIR and XRD, respectively, further demonstrates that a direct reaction between the mixed amide and hydride has occurred, resulting in the imide-like structure.
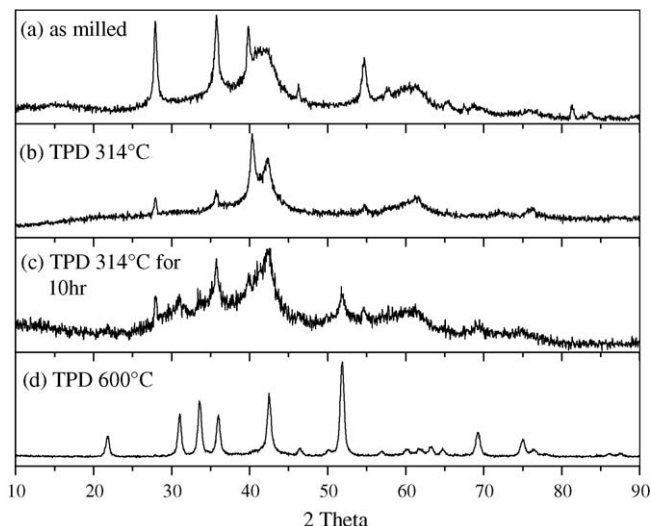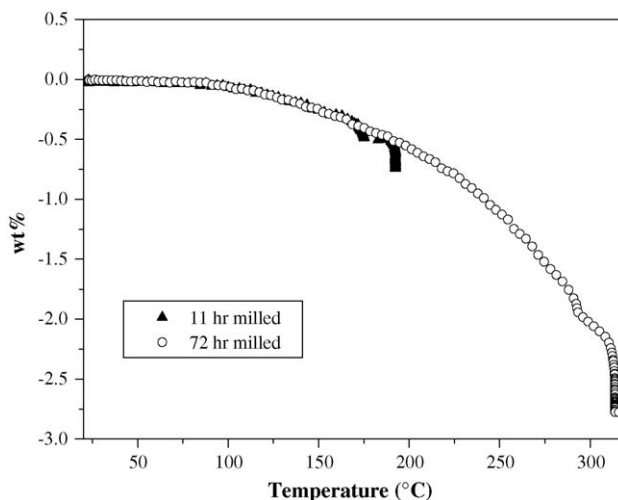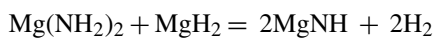
4. Conclusions

The ball-milling of $Mg(NH_2)_2$–MgH_2 mixture substantially changed the thermal decomposition behaviors of the individual components. The H_2 release from the amide–hydride reaction could be promoted by thorough ball-milling. The as-prepared samples released H_2 beginning at temperatures as low as 65 till 310 °C with a total amount of 4.8 wt.% of H_2 from the investigated system.

Fig. 9. XRD patterns of 72 h milled sample after TPD treatments.

Acknowledgements

References

[1] P. Chen, Z.T. Xiong, J.Z. Luo, J.Y. Lin, K.L. Tan, Nature 420 (2002) 302–304.

[2] P. Chen, Z.T. Xiong, J.Z. Luo, J.Y. Lin, K.L. Tan, J. Phys. Chem. B 107 (2003) 10967–10970.

[3] T. Ichikawa, S. Isobe, N. Hanada, H. Fujii, J. Alloy. Compd. 365 (2004) 271–276.

[4] Y. Nakamori, S. Orimo, Mater. Sci. Eng. B: Solid State Mater. Adv. Tech. 108 (2004) 48–50.

[5] Z.T. Xiong, G.T. Wu, J.J. Hu, P. Chen, Adv. Mater. 16 (2004) 1522–1525.

[6] Z.T. Xiong, J.J. Hu, G.T. Wu, P. Chen, J. Alloy. Compd. 395 (2005) 209–212.

[7] H.Y. Leng, T. Ichikawa, S. Hino, N. Hanada, S. Isobe, H. Fujii, J. Phys. Chem. B 108 (2004) 8763–8765.

[8] W.F. Luo, J. Alloy. Compd. 381 (2004) 284–287.

[9] US Patent 60/571,804, filed on May 17 (2004).

[10] Abstract Book of ASM Materials Solutions Conference and Show, 18–21 October 2004, Columbus, USA, 2004.

[11] Y. Nakamori, G. Kitahara, S. Orimo, J. Power Sources 138 (2004) 309–312.

[12] E. Akiba, Curr. Opin. Solid State Mater. Sci. 4 (1999) 267–272.

[13] J. Huot, G. Liang, R. Schulz, Appl. Phys. A: Mater. Sci. Process. 72 (2001) 187–195.

[14] Y. Kojima, Y. Kawai, Chem. Commun. (2004) 2210–2211.

[15] H.G. Schimmel, M.R. Johnson, G.J. Kearley, A.J. Ramirez-Cuesta, J. Huot, F.M. Mulder, J. Alloy. Compd. 393 (2005) 1–4.

[16] N. Hanada, T. Ichikawa, H. Fujii, J. Phys. Chem. B 109 (2005) 7188–7194.

[17] Z. Xiong, P. Chen, G. Wu, et al., J. Mater. Chem. 13 (2003) 1676–1680.

[18] J. Huot, G. Liang, S. Boily, A. Van Neste, R. Schulz, J. Alloy. Compd. 295 (1999) 495–500.

[19] G. Linde, R. Juza, Z. Anorg. Allg. Chem. 409 (1974) 199–214.